



Development of model for studies on momentum transfer in electrochemical cells with entry region coil as turbulence promoter

Tamarba Penta Rao, Ph.D in Chemical Engineering¹ · P. Rajendra Prasad¹

Received: 17 December 2017 / Accepted: 6 March 2018 / Published online: 13 April 2018
© The Author(s) 2018

Abstract

Entry region swirl promoters gain importance in industry because of its effectiveness in augmentation of mass and heat transfer augmentation. Design of equipment needs momentum transfer data along with mass or heat transfer data. Hence an experimental investigation was carried out with coaxially placed entry region spiral coil as turbulence promoters on momentum transfer in forced convection flow of electrolyte in circular conduits. Aqueous solution of sodium hydroxide and 0.01 M equimolar Ferri-ferro cyanide system was chosen for the study. The study covered parameters like effect of pitch of the coil, effect of length of the coil, diameter of the coil, diameter of the coil wire, diameter of the annular rod. The promoter is measured by limiting current technique using diffusion controlled electrochemical reactions. The study comprises of evaluation of momentum transfer rates at the outer wall of the electrochemical cell. Pressure drop measurements were also made to obtain the energy consumption pattern. Within the range of variables covered. The results are correlated by the momentum transfer similarity function. Momentum transfer coefficients were evaluated from measured limiting currents. Effect of each parameter was studied in terms of friction factor. A model was developed for momentum transfer. The experimental data on momentum transfer was modeled in terms of momentum transfer function and Reynolds number, geometric parameters.

Nomenclature

A	Area of electrode (m ²)
C	Constants of correlations of equations
C	Concentration of electrolyte (kg-mole/ m ³)
CL	Length of the conduit (m)
d	Diameter of the conduit (m)
d _e	Equivalent diameter of the conduit (d-d _i) (m)
D	Diffusion coefficient (m ² /s)
D _c	Diameter of the coil (m)
D _w	Diameter of the coil wire (m)
D _i	Diameter of the annular rod (m)
D _e	Eddy diffusivity (m ² /s)
F	Faraday's constant = 96,540 (coulombs/g-mole)
I _L	Limiting current density (amp)
k _L	Mass transfer coefficient (m/s)
L _c	Length of the coil (m)
N	Mass flux
P _c	Pitch of the coil (m/turn)

R	Radius of the conduit (m)
u _i	Velocity at the interface (m/s)
u _b	Average velocity (m/s)
u*	Friction velocity($\sqrt{\tau_0/\rho}$)
u _i ⁺	Dimensionless velocity (u/u*)
u _b ⁺	Dimensionless bulk velocity
u _m ⁺	Average fluid velocity (m/s)
v _m	Superficial velocity (m/s)
y	Coordinate distance normal to wall (m)
y ₁	Distance from wall at which u = u _b
y ₁ ⁺	dimensionless distance (y ₁ u*/ν)

Dimensionless

f	Friction factor
Re _m ⁺	Roughness Reynolds number for homogeneous flow
R	Roughness Momentum Transfer
(h ⁺)	
St	Stanton number
Sc	Schmidt number
Φ	Ratio between total of molecular and eddy viscosity and total of molecular and eddy diffusivity (ν _t /D _t)
Φ ₁	P _c /d _e
Φ ₂	L _c /d _e
Φ ₃	D _c /d _e
Φ ₄	D _w /d _e
Φ ₅	D _i /d _e

✉ Tamarba Penta Rao, Ph.D in Chemical Engineering
praophd@gmail.com

¹ Department of Chemical Engineering, Electro Chemical Research Laboratory, A. U. College of Engineering (A), Andhra University, Andhrarrrr Pradesh, Visakhapatnam 530003, India

n Numbers of ions transferred
 η Performance factor

Greek symbols

τ Shear stress (kg/ms^2)
 μ Viscosity of the fluid (poise)
 ρ Density of the fluid (kg/m^3)
 τ_0 Wall shear stress (kg/ms^2 , $f/2 \cdot \rho \cdot u_b^2$)
 ν Kinematics viscosity
 ν_e Eddy kinematics viscosity

Subscripts

b Buffer
 i Interface
 o Wall
 p Based on particle diameter
 t Total of molecular and eddy
 v Viscous
 V-b Viscous buffer region

1 Introduction

Augmentation of heat and mass transfer processes are never ending quest for an engineer or technologist. Augmentation of a transfer processes offer the following advantages. Increased throughputs for a particular size of an equipment or reduced size of equipment for a particular flow rate. The other advantages are less floor area, ease in handling of raw material and utilities. These factors leads to the reduction unit product cost. Hence the augmentation technique found attractive for researchers. To arrive at this above objective, several strategies have been followed. Efforts have been continued with the investigation being directed towards achieving energy- efficient mass transfer cells with assembly of the coils. The earliest augmentative technique is surface roughness [1] several works were reported in literature. Use of baffles [2] and surface alternations also come under this section. Works like spheres [3], fins [4], bluff bodies [5] and stream lined bodies [6] placed across the flow were also extensively found in literature. Flow through ducts and arched channels [7], jets [8] were also encountered. Investigations on insert promoters in heat and mass transfer operations were reported extensively. The work reported was on concentric rod placed in the circular conduit, since then heat and mass transfer studies with coaxially placed turbulence promoters were reported extensively. The investigation on co-axially placed promoters like twisted tapes [9], tapes wound on a rod [10], spiral coils [11], string of spheres [12] and cones [13], discs [14], orifices [15], circular rings places on a rod [16] were also studied. But works found in literature seemed to increase friction there by higher operating costs. This is particularly true for string of spheres, string of cone, string of discs [14], and flow past cylindrical rod [17],

across stream lined bodies [18], and many devices like axially displaced promoters, and surface modifiers.

In the present study an effort is made in acquiring higher augmentation rate with lower frictional losses. It will lead to the construction of energy efficient transfer operation. Several researchers employed swirl flow for the augmentation of their process. Therefore an attempt is made to employ swirl motion in achieving this objective swirl flow devices were incorporated in circular conduits and found their effectiveness on heat and mass transfer processes. Among the swirl generating devices twisted tapes [19], tapes wound on a rod [10], spiral coils [11], spiral coils placed on central rod of an annular conduits [20] and tangential entry of fluid are prominent. Among the coaxially placed promoters, Entry region swirl generating promoters received the attention of several researchers. Nageswara Rao V [21] employed tape, tape-disc assembly as turbulence promoters in their study. Murali Mohan et al. [22] used entry region coil and coil-disc assembly as turbulence promoters in circular conduits generated useful data for the augmentation. Present investigation is directed towards achieving energy efficient transfer process. To that effect, it envisaged to obtain mass transfer data at the inner wall of annular conduits along the length of the column. Subsequently, local mass transfer data were obtained and the results were reported. These results could be adopted for enhancing mass transfer processes like electro dialysis [23], ultra filtration [24], reverse osmosis [25] and several other processes and reported increased transfer rates. The electrochemical processes like electro winning [26], electro refining [27], electro milling [28] and electro organic synthesis [29] could employ swirl generating promoters to obtain higher transfer rates. Swirl flows have wide range of applications in various engineering areas such as chemical processes like mechanical mixing and separation devices, combustion chambers, turbo machinery, rocketry, etc. It can be effectively used in heat and mass transfer enhancements. In view of these observations, the present research work is momentum transfer data are experimentally obtained in the presence of electrochemical cells with entry region coil as turbulence promoter. It deals with the presence of the momentum transfer rate at the wall through limiting current technique.

The study is carried out to obtain the following information.

1. To obtain limiting currents data on the outer wall of an annular conduits with entry region coil as turbulence promoters.
2. To study the effect of geometric parameters on mass transfer namely - pitch of the coil (P_c), length of the coil (L_c), diameter of the coil (D_c), diameter of the coil wire (D_w), and diameter of the annular rod (D_i) on the outer wall momentum transfer coefficients.
3. To generate pressure drop data with insert promoters and to identify the effect of geometric parameters such as pitch of the coil (P_c), length of the coil (L_c), diameter of the coil (D_c), diameter of the coil wire (D_w), and diameter of the annular rod (D_i).

- To develop generalized correlations for momentum transfer in homogeneous flow.

The following information is derived out of the study.

- Momentum transfer coefficient is increases with increasing in velocity.
- Friction factor values are increasing with increase in pitch of the coil.
- Momentum transfer is increasing monotonously with increase in length of the coil.
- The effect of momentum transfer coefficient on the diameter of the coil has marginal effect on friction factor in the present study.
- Correlations were developed based on semi theoretical considerations. Wall similarity concept is used in the development of correlations. The following Correlation developed for momentum transfer is presented as:

Homogeneous flow

$$R(h^+) = 18648 [\text{Re}_m^+]^{-1} (Fr)^{0.495} \left(\frac{D_w}{d_e}\right)^{0.77} \left(\frac{D_i}{d_e}\right)^{-0.175} \quad (1)$$

This equation is useful for the design and development of energy efficient transfer processes.

2 Experimentation

The Schematic diagram of experimental set up is shown in Fig. 1. It was essentially consisted of a recirculation tank, an entrance calming section (A), a test section (B), and an exit calming section (C), thermo wells (E_1, E_2), flanges (F_1, F_2), gland nuts (G_1 to G_4), coiled copper tube (H), pump (P), rotameter (R), recirculation tank (T), U-tube manometer (UM) and valves (V_1 to V_5).

The recirculation tank was a cylindrical copper vessel of 100 l capacity with a drain pipe and a gate valve (V_1) for periodical cleaning of the tank. A copper coiled tube (H) provided with perforations. The perforations were meant for bubble of nitrogen through the electrolyte. The bubbling of nitrogen through the electrolyte expels the dissolved oxygen present if any. The tank was connected to the pump with a 0.025 m diameter copper pipe on the suction line of the centrifugal pump. The suction line was also provided with a gate valve (V_2). The discharge line from the pump divided into 2 lines. One line served as a bypass and a controlled by valve (V_3) is incorporated in it. The other line was connected to the entrance calming section (A). A control valve (V_4) and a

rotameter were also incorporated in the line. The control valve was used to regulate the flow of electrolyte. The rotameter served as flow measuring device. The rotameter has a range of 0 to $347 \times 10^{-6} \text{ m}^3/\text{s}$. The entrance calming section was circular copper pipe of 0.046 m ID provided with a flange and closed at the bottom with a gland nut (G_1). To an extent of 0.1 m of entrance calming was filled with capillary tube to damp the flow fluctuations and to facilitate steady flow of the electrolyte through the test section.

The details of the test section are shown in Fig. 2. It was made of a graduated perspex tube of 0.68 m length with point electrodes fixed flush with the inner surface of an outer wall of the test section. The point electrodes were made out of a copper rod and machined to the size. The electrodes were fixed flush with the inner surface of the outer wall of the test section at an equal spacing of 0.0254 m. The diameter of the exit calming section was also of the same diameter. The entrance calming section made of copper tube of 1.8 m long, and it was provided with a flange on the upstream side for assembling with the test section. The exit calming is also made of copper tube of length 0.7 m and diameter of 0.046 m. The exit and entrance calming sections were provided with gland nuts (G_2, G_3) at the top and bottom ends. The column comprised of 3 sections namely the entrance calming section, the test section and the exit calming section. These sections were assembled by means of flanges F_1, F_2 . Two thermo wells (E_1, E_2) were provided, one at upstream side of the entrance calming section and the other at the downstream side of exit calming section to measure the temperature of the electrolyte.

The coil is fixed at the entrance of the test section with the help of flanges. And the central rod is placed inside the column from top to bottom. The entry region coil was a spiral coil made from a copper wire of 0.006, 0.007, 0.008 m diameters. The copper wire was coiled to obtain coil diameters of 0.031, 0.034 and 0.038 m. The pitches of the coils were varied as 1.6, 2.6, 3.6, 4.6 cm. The spiral coil was welded to a flange. The flange has a matching perforation with that of test section. It is placed concentrically in the test section and fixed via flanged joints. The range of variables covered in a homogeneous flow of fluid is presented in Table 1.

Multimeter of Motwane make with accuracy of 0.01 mA was used as an ammeter and another multimeter was acted as voltmeter and has an accuracy of 0.01 V. They were used for measuring the limiting currents and potentials respectively. The other equipment used in circuit was rheostat, key, commutator, selector switch and a lead acid battery. The battery served as the power source. The commutator facilitated to reverse the polarity. The measurement of limiting currents for reduction process was taken. The selector switch facilitated the measurements of limiting currents at any desired electrode. Details of the coil assembly promoter covered in a homogeneous flow of fluid are presented in Table 2.

The limiting current data were obtained for the case of reduction of ferricyanide ion in annular conduit in the

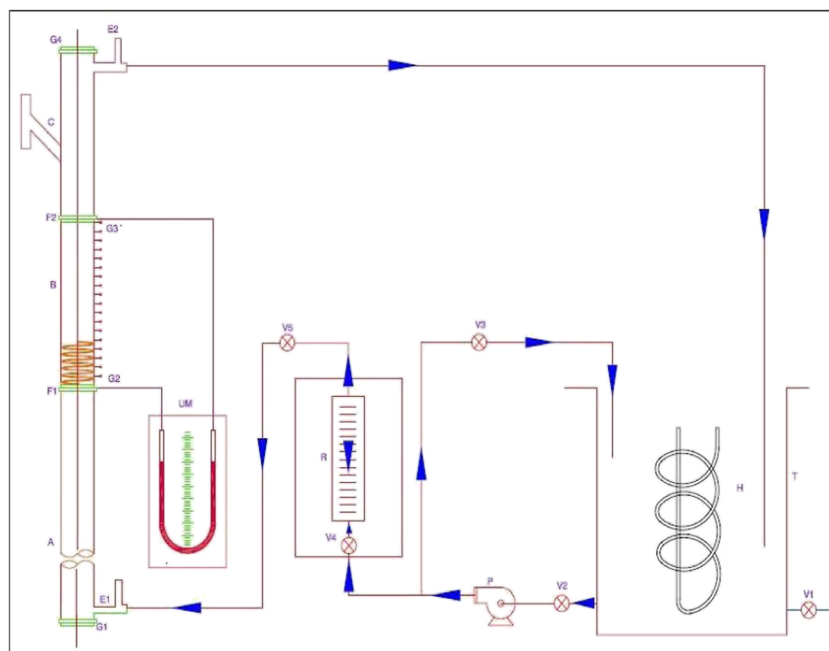
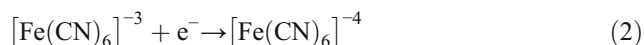


Fig. 1 Schematic diagram of the experimental set up. A: Entrance calming section. B: Test section. C: Exit calming section. E₁, E₂: Thermo wells. G₁ to G₄: Gland nuts. F₁, F₂: Flanges. H: Coiled copper tube. P: Pump. R: Rota meter. T: Recirculation tank. UM: U tube manometer. V1 to V5: Valves

presence of entry region coil as insert promoters in homogeneous flow. The cathodic reduction reaction of ferricyanide ion at the reacting electrode is given below



Eighty liters of equimolar solution of 0.01 N Potassium ferricyanide and 0.01 N Potassium ferrocyanide with 0.5 N Sodium hydroxide as electrolyte was prepared used as the system. The electrolyte was analyzed for ferrocyanide ion concentration by volumetric titration method using standard potassium permanganate solution [1] and for ferricyanide ion using idometric method [2]. The viscosity of the solutions at different temperatures were measured with Ostwald Viscometer and densities were measured using specific gravity bottle. The point electrodes in the test section were polished using four zero emery to get a smooth surface followed by degreasing with trichloroethylene solution. The size of the electrode was measured with a traveling microscope. After fixing the promoter in position, blank runs i.e. were conducted with sodium hydroxide electrolyte alone to ensure that the limiting currents obtained were due to diffusion of reacting ions (Ferricyanide ion) only. Subsequently, known quantities of potassium ferricyanide and potassium ferrocyanide were added to get the concentration of electrolyte was maintained at equimolar 0.01 M Ferri-ferrocyanide couple was maintained.

The coils of known geometry were fitted at the entrance of the test section by means of flanged joint and the annular rods were fixed by means of gland nuts. The experiments were repeated by replacing the coil and /or annular rod. The electrolyte was pumped at a desired flow rate (through the test section) by

operating the control and by-pass valves. After the steady state was attained, potential was applied across the test electrode and wall electrode in small increments of potential (100 mV) and the corresponding current values were measured for each increment. As the area of the wall electrode was relatively large in relation to the area of the test electrode, nearly constant potential was obtained at the test electrode. Since the potential values are not of criteria in the present study, the limiting currents only were obtained from the current and potential data.

The experiment was repeated by changing the flow rate of the electrolyte and the limiting currents measurements were taken for each flow rate. Measurement of limiting current: The plots of current versus potential data yields limiting currents. Increase in potential increases the current up to certain value and further increase in potential would be maintained nearly constant current values, which is taken as the limiting current. Mass transfer coefficients are computed from the measured limiting currents by the following expression:

$$k_L = \frac{i_L}{n F A C_o} \quad (3)$$

Pressure drop measurements for each flow rate were made simultaneously by using a U – tube manometer with Carbon tetrachloride as manometer liquid.

3 Results and discussions

Experiments were conducted with entry region coil promoter assembly in a homogeneous flow of electrolyte. It

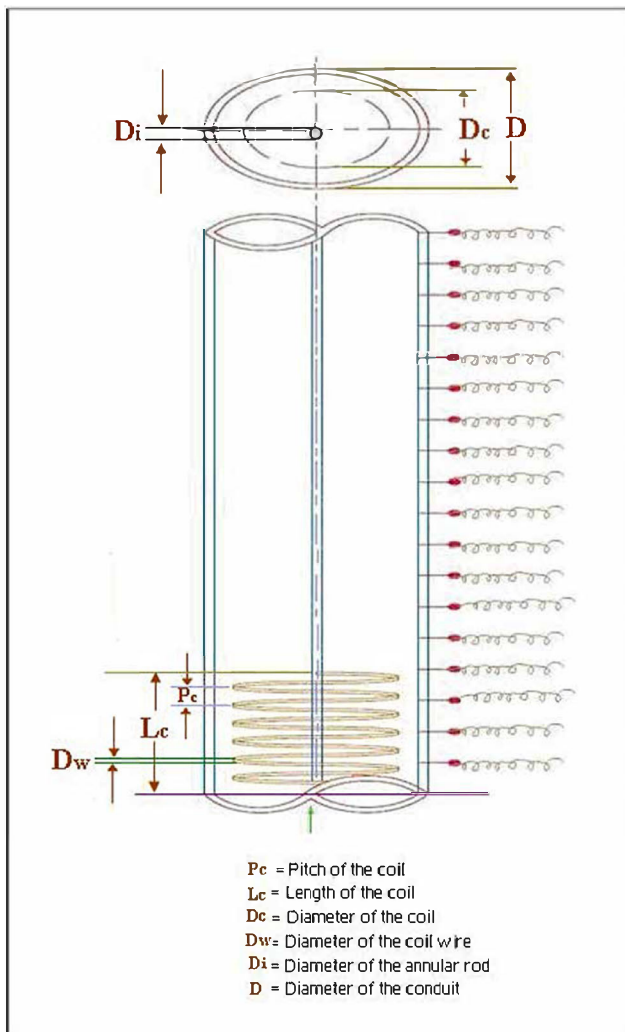


Fig. 2 Details of the test section

deals with 7500 local limiting current data obtained at the outer wall of an annular conduit fitted with an entry region spiral coil as a turbulence promoter. Local limiting currents at the outer wall of an annulus were measured along the length of the column. Cathodic reduction of ferricyanide ion was chosen as the system for the present study.

Table 1 Range of variables covered in the present study

Variables	Minimum	Maximum
Pitch of the coil (P_c), m/tum	0.016	0.046
Length of the coil (L_c), m	0.05	0.16
Diameter of the coil (D_c), m	0.031	0.038
Diameter of the coil wire (D_w), m	0.006	0.008
Diameter of the annular rod (D_i), m	0.0127	0.0254
Reynolds number, Re	1200	14,500
Schmidt number, Sc	789	1132

Table 2 Details of the coil assembly promoter covered in the present study

Pitch of the Coil (P_c), m:	0.016, 0.026, 0.036, 0.046
Length of the Coil (L_c), m:	0.05, 0.09, 0.12, 0.16
Diameter of the Coil (D_c), m:	0.031, 0.034, 0.038
Diameter of the coil wire (D_w), m:	0.006, 0.007, 0.008

3.1 Studies on homogeneous flow with entry region coil in annular conduits

The experimental measurements consists of the flow rate of an electrolyte (Q), limiting current (i_L). From the measured current potential data, limiting currents were identified. The concentration of reacting ion (C_o) was estimated by isometric. Physical properties of the solution namely density (ρ), viscosity (μ) were measured by suitable method. The values of Diffusivities (D_L) were estimated by the method mentioned in experimental procedure. Diameter of the test section (d) and dimensions of the promoter assembly viz., pitch of the coil (P_c), length of the coil (L_c), diameter of the coil (D_c), diameter of the wire of the coil (D_w), diameter of the annular rod (d_i) and temperature (T), were measured with suitable instruments.

The velocity of the fluid flow was computed from the following expression.

$$V = \frac{Q}{\frac{\pi}{4}(d_e^2)} \quad (4)$$

Where $d_e = (d - D_i)$ is equivalent diameter.

3.2 Momentum transfer

Entry region coil induces swirl in the flowing fluid as the fluid passes through an annular conduits which is fitted with an entry region spiral coil. As the fluid moves along the coil, the fluid elements are guided by the coil and are transformed from the axial flow into swirl flow. The swirl approaches to a maximum value. The fluid elements leaves the coil with maximum swirl velocity followed a decaying zone due the absence of the coil. The swirl continues to some extent followed by a decaying zone. As we move along the length of the column the flow slowly transform from swirling flow to axial and finally the flow reaches smooth conduit flow without any promoter. Because of the induced swirl motion changes in pressure drops are anticipated higher. Sufficient study in this direction is not made so far. Therefore pressure drop measurements were also made along with mass transfer data. The effective friction factor values are computed from the measured pressure drops by the following equation for homogeneous flow.

$$f = \frac{\Delta P d_e g_c}{2 L V^2 \rho} \quad (5)$$

Based on friction factor versus Reynolds number data one can analyze the energy losses. The information is highly useful in the design and development of energy efficient electrochemical cells. The frictional losses are directly related to the flow condition prevailed in the column. These friction factor data would be useful in the analysis of mass transfer data which is analyzed in terms of geometric parameters of the promoters.

3.3 Effect of pitch of the coil

To show the effect of coil pitch, the data of friction factor versus Reynolds number for 4 coils with different pitch are plotted and shown in Fig. 3. The figure reveals the friction factor values are increasing with increase in Reynolds number and converging at a higher velocity end. Further increase in velocity might lead to convergence and would result in the formation of fully turbulent region i.e. the friction values becomes constant.

It is further observed that at any velocity within the range of variables covered in the present study, friction values are increasing with increase in pitch of the coil. The increase would continue up to certain pitch, on further increase in pitch would result in decrease in pitch because of the reduction in number of turns and thereby blockage or due to the reduction in cross flow element. Such pitch may be called a critical pitch. Similar observations were also made in mass transfer and by several other works [11, 20, 30, 31, and]. The early observation of this critical pitch is seen in mass transfer which may be an indication that the energy spent in the generation of turbulence is not fully utilized to augment mass transfer.

3.4 Effect of length of the coil

As length of the coil increases the generated swirl is more prominent. Increased coil length consumes more pressure force reducing the superficial velocity of the fluid therefore enhanced friction factors; this observation coincides with mass transfer. A graph is drawn for friction factor versus Reynolds number for the coils having the same pitch and different coil lengths and shown as Fig. 4. Friction factor values are found to decrease with Reynolds number. Friction

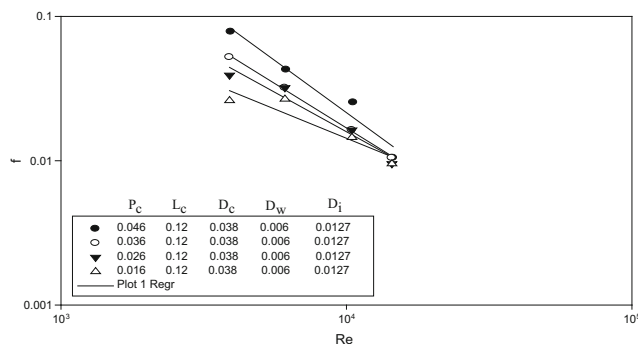


Fig. 3 Variation of f – Effect of pitch of the coil

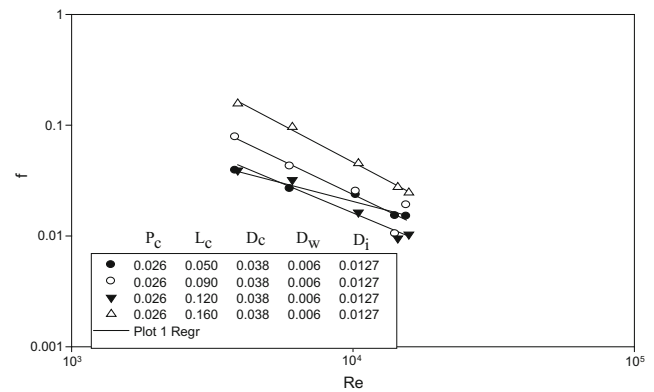


Fig. 4 Effect of length of the coil on friction factor

factor values are increasing with the length of the coil but for the coil length 12 cm. It is an exception where the friction values are low within the range of variables studied. For better performance the coil with length 12 cm is recommended. But the reason for the decrease is not clearly understood.

3.5 Effect of coil diameter

A graph is drawn as f versus Re and shown in Fig. 5. Diameter of the coil has marginal effect on friction factor. Friction factor values are increasing marginally with diameter of the coil. The diameter of the coil could not be varied much because of narrow gap between annular rod and wall of the test section.

3.6 Effect of the diameter of the coil wire diameter

Diameter of the coil wire has significant effect on friction factor. Its effect could be seen from Fig. 6. The values of f are decreasing with Reynolds number (Re). The slope is steep for the coil wire diameter of 0.008 m. On further increase in Re a sharp increase is followed at higher Re . At lower flow rates the coil wire diameter 0.06 is recommended.

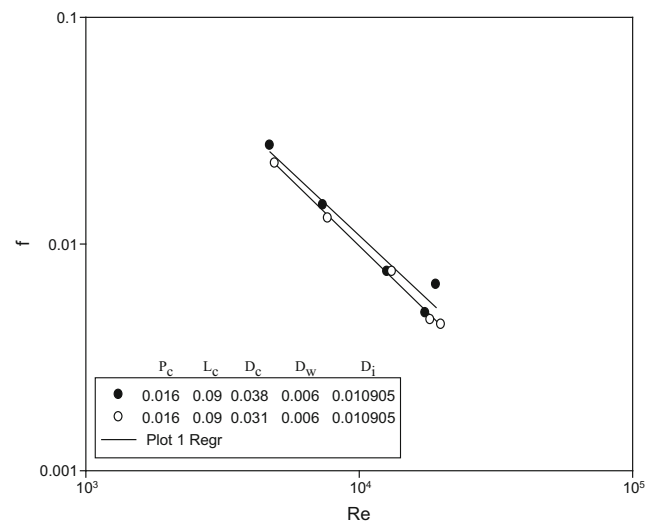


Fig. 5 Effect of coil diameter on friction factor

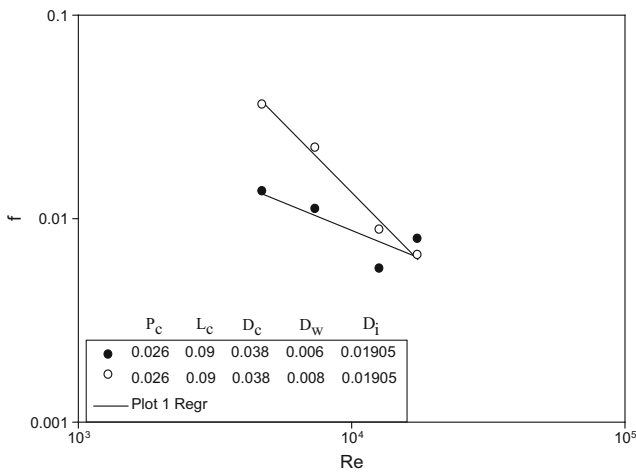


Fig. 6 Effect of coil wire diameter on friction factor

3.7 Energy enhancements over the data of smooth pipe flow

The energy requirement for unit area of the cell is calculated by the following equation.

$$E = \frac{Q \Delta P}{(\prod d L + \prod d_i L)}$$

The energy loss in the case of pipe without any insert in them is indicated by E_0 . The energy factor is defined as E/E_0 . A graph is drawn as energy factor versus Reynolds number and presented as Fig. 7. These figures reveal energy factors are decreasing with Reynolds number.

3.8 Performance of the entry region coil promoter

Performance factor (η) is the ratio of augmentation factor to energy factor and defined by the following equation.

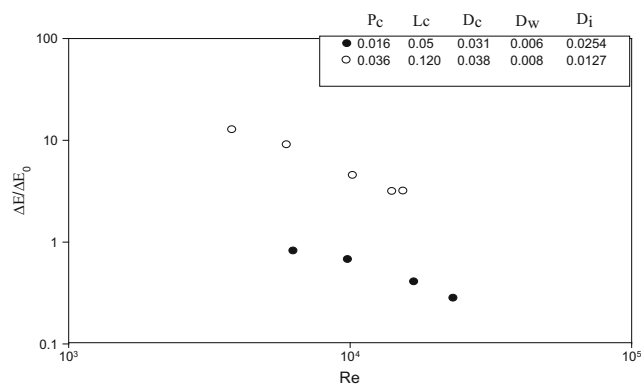


Fig. 7 Variation of augmentation factor with Reynolds number

$$\eta = \frac{k_L/k_{L0}}{E/E_0} = \frac{k_L/k_{L0}}{\Delta P/\Delta P_0}$$

A graph is drawn energy factor with Reynolds number for 2 different sets with coils of varying geometric configuration as shown in inset and shown as Fig. 7. The figure reveals the energy factor is decreasing with Reynolds number. Further increase in Reynolds number would remain constant which is could be seen when range flow rate increased further. The efficiency (η) is a measure for efficiency of the promoter. Efficiency of the promoters under study could be judged from graphs of Performance factor versus Reynolds number. A graph is drawn as performance factor versus Reynolds number and shown as Fig. 8. The Performance is increasing linearly with Re. The promoter producing maximum turbulence is augmenting better and the efficiencies are increasing steeply indicating higher augmentation at lower flow rates.

4 Development of generalized correlations

4.1 Momentum transfer

Flow of electrolyte through circular conduit with entry region spiral coil promoter generates a variety of flow fields. The development of momentum transfer correlations for the present situation could be carried out on the basis of semi empirical data. Conventional $f - Re$ type correlations have been attempted to correlate the present data using the following format of equation.

$$f = C Re^m (\Phi_1)^{n_1} (\Phi_2)^{n_2} (\Phi_3)^{n_3} \tag{6}$$

Where Φ_1, Φ_2, Φ_3 are the geometric parameters. Regression analysis of the data in accordance with the above format of equation yielded the following correlations for the data for

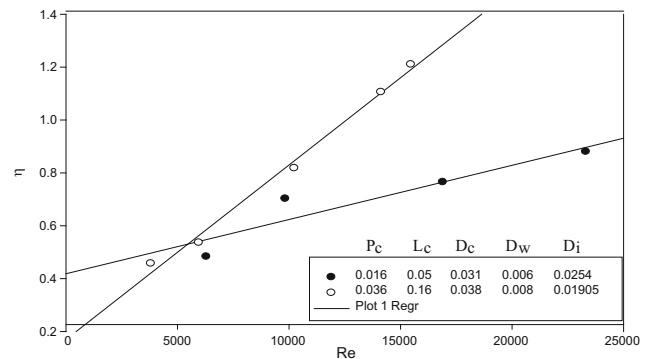


Fig. 8 Variation of effectiveness factor with Reynolds number

flow through annular conduits with entry region coil as insert resulted high deviations.

$$f = 10.9\text{Re}^{-0.203}(P_c/d)^{-0.44}(L_c/d)^{0.56}(D_c/d_e)(D_w/d_e) \quad (7)$$

In view of these large deviations, an alternative approach has been attempted by the use of the wall similarity concept proposed by Webb, R, L et al. [1], Dippery and Saborsky [32], Nikuradse, J [33] and Deissler R G [34]. The similar concept assumes velocity distribution is expected to experience the effect of viscosity at the surface. When an object is placed across the flow in a circular conduit, drag is generated and the drag enhances turbulence. Thus generated turbulence exerts tractive force at the wall and makes the boundary layers thinner. The flow is divided into 2 regions namely inner region and outer region. The inner region constituted with boundary layer whose thickness is δ at y^+ , where δ is small. The velocity distribution depends on y^+ , τ_0 , μ .

For inner region the velocity profile in terms of dimensionless velocity is given by

$$u^+ = y^+ \quad (8)$$

Where $u^+ = u/u^*$, $y^+ = yu^*/\nu$, For the outer wall region where the dependency of velocity distribution on molecular viscosity ceases to exist, the velocity distribution would follow the relationship

$$u^+ = \frac{1}{k} \ln y^+ + C_1 \quad (9)$$

By the application of boundary conditions $u = 0$ at $y = y_0$, where y_0 is the thickness of laminar sub layer that depends on the turbulence generated, Eq. 9 reduces to

$$u^+ = \frac{1}{k} \ln(y/y_0) \quad (10)$$

The turbulence in the core and at the wall is significantly affected by the geometric parameters of the promoters employed in addition to the fluid velocity. In the present case, Pitch of the coil (P_c) and Length of the coil (L_c), diameter of the coil (D_c), diameter of the coil wire (D_w), and annular rod (D_i) are the major characteristic geometric parameters. As these are expected to be significantly affect the thickness of the laminar sub layer. In the present study the parameter (D_w), was chosen while computing u^+ therefore,

$$y_0 \propto D_w \quad (11)$$

Equation 10 could be modified as

$$\frac{u_{\max} - u}{u^*} = \frac{1}{k} \ln(y/D_w) \quad (12)$$

Combination of Eqs. 11 and 12 gives the velocity distribution equation for the turbulent dominated part of the wall region

$$u^+ = 2.5 \ln[y/D_w] + R(h^+) \quad (13)$$

The above equation presents modified velocity profile for the case of out turbulent region in the presence of promoters. Assuming that Eq. 14 holds good for the entire cross section of the circular conduit, the friction factor for the turbulent flow with entry region coil inside the annular conduit can be given by integration of Eq. 13. The generated roughness function $R(h^+)$ is given by the following equation

$$R(h^+) = 2.5 \ln[2(D_w)/d_e] + \sqrt{2/f} + 3.75 \quad (14)$$

Where $R(h^+)$ is roughness momentum transfer function, This type of analysis is followed by the earlier workers (11, 23, 24) and successfully analyzed their data.

The resulting format of equation for correlating the momentum transfer data with entry region spiral coil as promoter in annular conduits can now be written as

$$R(h^+) = C_1 [\text{Re}_m^+]^{b_1} \quad (15)$$

Here, C_1 is proportionality constant and b_1 is an exponent, Re_m^+ is roughness Reynolds number defined by the following equations for entry region coil with annular conduits in homogeneous flow. The analysis could also be useful for fluidized beds with modification of particle Reynolds number defined in following text.

4.2 Homogeneous flow

Data on homogeneous flow is analyzed in terms of in terms of $Rh^+ v_s \text{Re}_m^{+s}$

$$R(h^+) = 2.5 \ln[2(D_w)/d_e] + \sqrt{2/f} + 3.75 \quad (16)$$

$$\text{Re}_m^+ = (D_w/d_e) \cdot \text{Re} \cdot \sqrt{f/2} \quad (17)$$

Where D_w is wire diameter, d_e is diameter of the conduit and f is friction factor. On regression analysis and by omitting geometric parameters of the promoter yielded the following equations.

$$R(h^+) = 206.73 [\text{Re}_m^+]^{-0.10}$$

Average deviation=39.816 Standard deviation=57.166 (18)

Multiple regression analysis was conducted with relevant geometric groups also resulted very high deviations. An attempt is made to include Froude group,

Where For homogeneous flow $\text{Fre} = V^2/(d_e \cdot g)$, (19)

The effect of Froude group is prominently appearing when ever vortex or swirl generating type of flow appears. The

regression analysis was conducted with $R(h^+)$ and with 2 dimensionless numbers namely Reynolds number and Froude group.

The resultant equations are also associated with large deviations.

$$R(h^+) = 3329.3 [Re_m^+]^{-0.866} [Fr]^{0.454}$$

Average deviation=7.4194 Standard deviation=8.7775
(20)

Hence other geometric groups were also included in the correlation. The correlations resulted were of good accuracy and with very marginal deviation. These correlations were presented hereunder

$$R(h^+) = 18648 [Re_m^+]^{-1} (Fr)^{0.495} \left(\frac{D_w}{d_e}\right)^{0.77} \left(\frac{D_i}{d_e}\right)^{-0.175}$$

Average deviation = 2.1639 Standard deviation = 2.6012
(21)

In Correlation graph for momentum transfer in homogeneous flow with entry region coil in annular conduits is presented along with the data of with that system in full length coils as turbulence promoters and can be seen in Fig. 9.

5 Comparison of correlation

Present correlation is tested for its ability to predict with other works. Typical data (the coil which augments best of full length coil is recalculated in the lines of present study and embedded in the present correlation graph shown as Fig. 10. The figure reveals, that the present correlation could predict well. The data of entry region coil in circular conduit is deviating moderately.

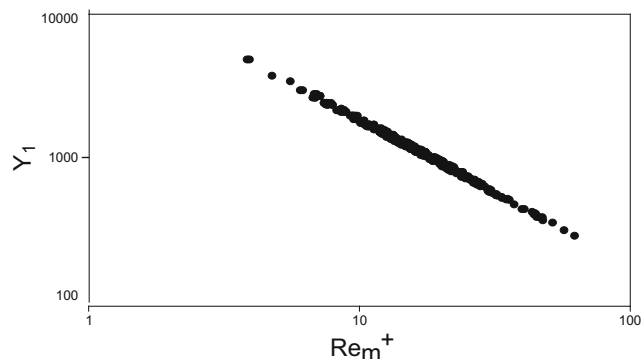


Fig. 9 Correlation graph for momentum transfer – homogeneous flow

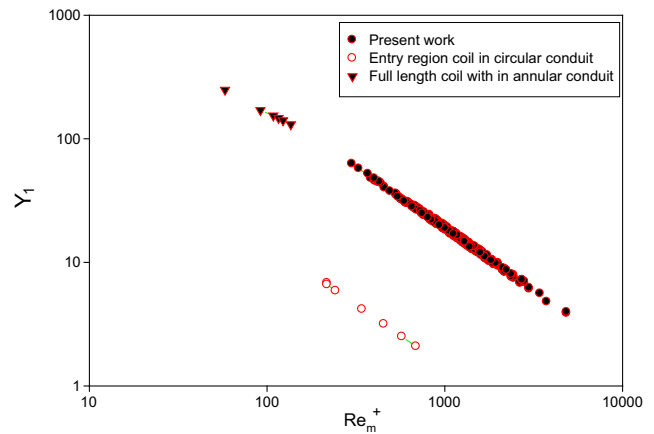


Fig. 10 Comparison graph for momentum transfer correlation in homogeneous flow

5.1 Efficiency of the promoter

A graph is drawn as efficiency versus volumetric flow rate and the figure reveal that the present work is clearly efficient than the presented in the Fig. 11.

6 Conclusions

The following conclusions can be drawn from the present analysis:

1. Friction factor values are increasing with increase in pitch of the coil.
2. Larger the length of the coil greater the frictional values.
3. Diameter of the coil has marginal effect on friction factor in the present study.
4. Greater the coil wire diameter larger the friction factors.
5. The energy factor values are decreasing with Reynolds number.

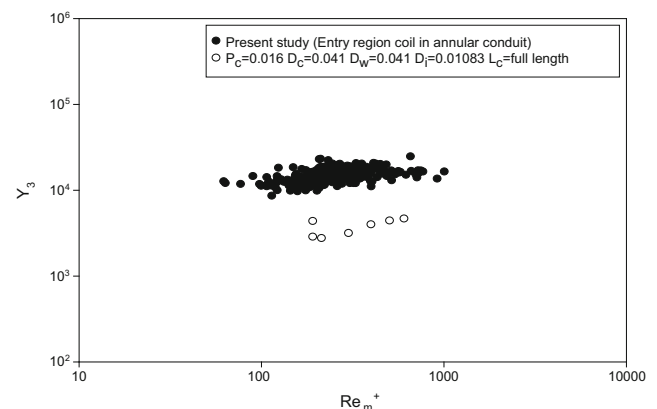


Fig. 11 Comparison graph for homogeneous flow in annular conduits

6. The Performance of the coils are increasing linearly with Re. The promoter producing higher turbulence is also augmenting better and the efficiencies are increasing steeply indicating higher augmentation at lower flow rates.
7. A Model developed for momentum transfer in homogeneous flow is as follows:

$$R(h^+) = 18648 [\text{Re}_m^+]^{-1} (Fr)^{0.495} \left(\frac{D_W}{d_e}\right)^{0.77} \left(\frac{D_i}{d_e}\right)^{-0.175}$$

Open Access This article is distributed under the terms of the Creative Commons Attribution 4.0 International License (<http://creativecommons.org/licenses/by/4.0/>), which permits unrestricted use, distribution, and reproduction in any medium, provided you give appropriate credit to the original author(s) and the source, provide a link to the Creative Commons license, and indicate if changes were made.

Publisher's Note Springer Nature remains neutral with regard to jurisdictional claims in published maps and institutional affiliations.

References

1. Webb RL, Eckert ERG, Goldstein RJ (1971) Heat transfer and friction in tubes with repeated-rib roughness. *Int J of Heat and Mass Transf* 14(4):601–617
2. Zheng M, Li J, Mackley MR (2007) The development of asymmetry for oscillatory flow within a tube containing sharp edge periodic baffles. *Phys Fluids* 19(11):114101–114115
3. Hong SW, Bergles AE (1976) Augmentation of laminar flow heat transfer in tubes by means of twisted-tape inserts. *J Heat Transf* 98(2):251–256
4. Hwa Won Ryu, Young Soon Hyeon, Dong II Lee, Ho Nam Chang, O Ok Park (1991) Pressure drop and mass transfer around perforated turbulence promoters placed in a circular tube. *Int J of Heat and Mass Transf* 34(8):1909–1916
5. Ravi T, Srinivasa Rao B, Gopala Krishna P, Venkateswarlu P (1996) Ionic mass transfer studies in fluidized beds with coaxially placed discs on a rod as internal. *Chem Eng Process* 35(3):187–193
6. Dawson DA, Trass O (1972) Mass transfer at rough surfaces. *Int J of Heat and Mass Transf* 15(7):1317–1336
7. Niu JL, Zhang LZ (2002) Heat transfer and friction coefficients in corrugated ducts confined by sinusoidal and arc curves. *Int J of Heat and Mass Transf* 45(3):571–578
8. Prasad VSRK (1994) Studies on ionic mass transfer with impinging jet in closed cylindrical cells. Ph.D. thesis. In: Andhra university. Visakhapatnam, India
9. Naphon P (2006) Heat transfer and pressure drop in the horizontal double pipes with and without twisted tape insert. *Int Comm in Heat and Mass Transf* 33(2):166–175
10. Sujatha V (1991) Studies on ionic mass transfer with coaxially placed helical tapes on a rod in homogeneous fluid and fluidized beds. Thesis, Andhra University, Visakhapatnam, India, Ph. D
11. Rajendra Prasad P (1993) Studies on ionic mass transfer with coaxially placed spiral coils as turbulence promoter in homogenous flow and in fluidized beds. Andhra University, Visakhapatnam, India, Ph. D Thesis
12. Sitaraman TS (1977) Augmentation of mass transfer with coaxial string of spheres as internals in tubes and fluidized beds. Ph.D. In: Thesis. University of Madras, India
13. Sarveswara Rao S (1983) Studies on ionic mass transfer with coaxially placed cones on a rod in homogeneous fluid and fluidized beds. Ph.D. In: Thesis. Andhra University, Visakhapatnam India
14. Venkateswarlu P (1987) Studies on ionic mass transfer with coaxially placed discs on a rod as turbulence promoter. Ph.D. thesis. In: Andhra university. Visakhapatnam, India
15. Kumari S (2003) Studies on mass transfer using coaxial- orifice turbulence promoters. Andhra University, Visakhapatnam, India, M. Tech Thesis
16. Chungal Raju D (1984) Augmentation of mass transfer at the outer wall of concentric annuli in presence of fluidizing solids-effect of wires wound on central rod. Ph. D. Thesis, Andhra University, Visakhapatnam, India
17. Bhaskar Sarma C (1978) Ionic mass transfer at circular and elliptical cylinders in cross flow of homogeneous fluid and in fluidized solids. Ph. D. Thesis, Andhra University, Visakhapatnam, India
18. Evans LB (1962) The effect of axial turbulence promoters on heat transfer. Ph.D. In: Thesis. University of Michigan, Michigan
19. Bhatia et al (1967) Studies on spiral coils, twisted tapes as turbulence promoters in their heat transfer and pressure drop. *J Inst of Engg India* 48(1):34–35
20. Chungal Raju D (1984) Augmentation of mass transfer at the outer wall of concentric annuli in absence and presence of fluidizing solids effect of wires wound on central rod. Ph.D. thesis. In: Andhra university. Visakhapatnam, India
21. Nageswara Rao V (2004) Studies on ionic mass and momentum transfer with co-axially placed twisted tape disc assembly as turbulence promoter in circular conduits. Ph.D. thesis. In: Andhra university. Visakhapatnam, India
22. Murali Mohan V (2008) Studies on mass and momentum transfer with coaxially placed entryregion coil, disc and coil-disc assembly as turbulence promoters in circular conduits. Ph.D. thesis. In: Andhra university. Visakhapatnam, India
23. Grigorchuk OV, Vasil'eva VI, Shaposhnik VA (2005) Local characteristics of mass transfer under electro dialysis demineralization. *Desali* 184(1–3):431–438
24. Venkateswarlu P, Jaya Raj N, Subba Rao D, Subbaiah T (2002) Mass transfer conditions on a perforated electrode support vibrating in an electrolytic cell. *Chem Engg and Proces* 41(4):349–356
25. Prabhakar S, Ramani MPS (1994) A new concept of mass transfer coefficient in reverse osmosis practical applications. *J Membr Sci* 86(1–2):145–154
26. Subbaiah T, Das SC (1994) Effect of some common impurities on mass transfer coefficient and deposit quality during copper electro winning. *Hydrometal* 36(3):271–283
27. Subbarao D, Venkateswarlu P (2004) Ionic mass transfer studies in an open cell in the presence of circular cylindrical promoters. *Chem Engg and Proces* 43(1):35–41
28. Goma H, Al Taweel AM, Landau L (2004) Mass transfer enhancement at vibration electrodes. *Chem Engg J* 97(2–3):141–149
29. Zaki MM, Nirdosh SN (2007) Mass transfer characteristics of reciprocating screen stack electrochemical reactor in relation to heavy metal removal from dilute solutions. *Chem Engg J* 126(2–3):67–77
30. Chiou JP (1987) Experimental investigation of the augmentation of forced convection heat transfer in a circular tube using spiral spring inserts. *Trans ASME* 109:300–307
31. Rajendra Prasad P, Sujatha V, Sarma CB, Raju GJVJ (2004) Studies on ionic mass transfer with coaxially placed spiral coils as turbulence promoter in homogenous flow and in fluidized beds. *Chem Engg and Proces J* 43:1055–1062
32. Dipprey DF, Sabersky RH (1963) Heat and momentum transfer in smooth and rough tubes at various prandtl numbers. *Int J of Heat and Mass Trans* 6(5):329–332
33. Nikuradse J (1933) Laws of flow in rough pipes. *VDI Forsch*, 361
34. Deissler RG (1955) Analysis of turbulent heat transfer, mass transfer and friction in smooth tubes at high Prandtl and Schmidt. *Nat Adv Comm Aeronaut*, Washington, DC TN-1210